Enhancement of Ferroelectric Curie Temperature in BaTiO₃ Films via Strain-Induced Defect Dipole Alignment

Anoop R. Damodaran, Eric Breckenfeld, Zuhuang Chen, Sungki Lee, and Lane W. Martin*

Significant advances in the growth and characterization of ferroelectric thin films have highlighted the role of substrate induced strain in enhancing ferroelectric properties.[1] This includes the observation of an enhanced ferroelectric transition temperature (T_C) in $BaTiO_3$,[2,3] room-temperature ferroelectricity in $SrTiO_3$,[4] and stabilization of highly-distorted polymorphs of $BiFeO_3$.[5] Despite considerable excitement over the potential of thin-film strain to control materials, it is fundamentally limited in a number of ways: 1) the magnitude of the strain that can be applied before the onset of relaxation is relatively small (generally <1% lattice mismatch), 2) the thickness of a coherently strained film must be maintained below a critical thickness for strain relaxation which often renders such strain-engineered films unsuitable for applications that require high voltages, and 3) there is a lack of continuous tunability arising from the limited number of substrates and the need to switch between them to change the strain state. In turn, these factors put rather stringent limits on our ability to manipulate the properties and enhance performance on demand in these materials. Despite these limitations, much work has illustrated the potential of epitaxial constraints in manipulating ferroelectric materials.

In spite of extensive work in this arena, there are a number of observations over the years that do not follow our fundamental understanding of thin-film strain. In $BaTiO_3$-based films, for instance, as early as the 1980s and 1990s researchers were reporting anomalously large lattice expansions in films,[6-9] especially those grown by highly-energetic growth processes such as sputtering, pulsed-laser deposition, etc., that were not commensurate with the pervasive understanding of epitaxially constrained $BaTiO_3$. For instance, rf sputtered $BaTiO_3$ films were found to exhibit lattice parameters as much as 8.6% larger than bulk versions (well beyond the expected 2.8% expansion of the c axis for a coherently strained $BaTiO_3$ film grown on $SrRuO_3/SrTiO_3$ (001) substrates).[9] A number of potential explanations were posited for these observations and, as early as 1983, researchers were suggesting that the observed distortions could not be explained by classic epitaxial strain alone. Instead, researchers hypothesized that an anisotropic distribution of point defects (namely interstitial atoms and vacancies) could be responsible for the added distortion.[7] In turn, a potential connection between the growth process and the observed lattice expansion has been proposed[7,10,11] and some have evoked the concept of "negative pressure" induced effects (i.e., large tetragonal strains and anomalous volume expansion under negative hydrostatic pressures)[12] to potentially explain the observations.[10] In turn, these anomalous lattice expansions are associated with interesting changes in the physical properties including enhancement of the ferroelectric transition temperature[7,11,13] and voltage-shifted ferroelectric hysteresis loops where the voltage shift scales linearly with thickness.[8,13,14] Despite this range of interesting work, no clear explanation for the effects has been developed, but it is generally considered that defects could play some role in the manifestation of these effects.

The study of defects in these complex materials is not new, but to really control these materials requires an intimate knowledge of the nature of defects that can occur.[15] While defects in ferroelectrics could potentially degrade the properties (i.e., worsening leakage and promoting aging)[16] and can also impact the structure, phase transitions, and polar ordering,[17,18] various defect-engineering strategies have been developed to alleviate such effects and have been widely used to control lifetimes of ferroelectric capacitors in switching-based applications as well as for tailoring the mobility of domain walls for piezoelectric applications.[16,19-21] Recent investigations have highlighted some unexpected benefits of specific defect-types, for instance, charged point defect complexes (so-called defect dipoles) have been utilized to achieve new functionalities including large reversible strains,[22] multistate memory effects,[23] and colossal dielectric responses.[24] In this work, we highlight how, when combined with thin-film epitaxy, the presence of such defect dipoles can give rise to enhanced ferroelectric ordering in materials and can explain many of the effects in $BaTiO_3$ noted above. By directly coupling the electrical and elastic dipoles of the defect complexes with the polarization and epitaxial strain state of the film, respectively, we can align the defects thereby inducing an additional anisotropic lattice deformation. Such a coupling of the elastic dipole of the defects with stress has been demonstrated before,[25-27] but here we develop a new paradigm in strain control of ferroelectric materials whereby we leverage

A. R. Damodaran, E. Breckenfeld, Z. H. Chen, S. Lee
Department of Materials Science and Engineering
and Materials Research Laboratory
University of Illinois
Urbana-Champaign
Urbana, IL 61801, USA
A. R. Damodaran, Z. H. Chen, L. W. Martin
Department of Materials Science and Engineering
University of California, Berkeley
Berkeley, CA 94720, USA
E-mail: lwmartin@berkeley.edu
L. W. Martin
Materials Science Division
Lawrence Berkeley National Laboratory
Berkeley, CA 94720, USA

this and the corresponding coupling with the primary order parameter of the material to enhance performance. We demonstrate that in BaTiO$_3$ films, known to possess a strong coupling between strain and polarization,[28] that deterministically controlling the electric- and elastic-dipole moments of engineered defect complexes allows us to systematically enhance the T_C to >800 °C without degradation of the polarization or leakage properties. This work highlights the potential of the combination of strain- and defect-engineering as a new route to control material properties.

130–170 nm BaTiO$_3$/40 nm SrRuO$_3$ thin-film heterostructures were grown on DyScO$_3$ (110), GdScO$_3$ (110), and NdScO$_3$ (110) single crystal substrates (corresponding to lattice mismatches with the pseudocubic lattice parameter of BaTiO$_3$ of −1.7%, −0.99%, and 0.08%, respectively) via pulsed-laser deposition (PLD) (see Experimental Section). The PLD process is complex and care must be taken to control the stoichiometry and defect structures in the resulting films.[29–31] The BaTiO$_3$ films were grown at laser fluences ranging from 1.5–2.7 J/cm^2 (details of laser fluence determination are provided in the Supporting Information). X-ray diffraction (XRD) studies reveal that all films are epitaxial and single phase (data for films grown on GdScO$_3$ substrates are provided, **Figure 1**a, and additional data is provided in the Supporting Information, Figure S1). Subsequent off-axis X-ray reciprocal space mapping (RSM) studies about the 103- and 332-diffraction conditions for the films and substrate, respectively, show that although the in-plane lattice parameters of the films are matched to that of the substrate, the out-of-plane lattice parameter of the BaTiO$_3$ increases as the laser fluence increases (Figure 1b–f, expected peak locations for bulk (B) and coherently strained (S) BaTiO$_3$ are indicated for comparison). From both Poisson and electrostriction effects an increase in the c-axis lattice parameter by 1.7% as compared to bulk is expected,

but in all films studied here an additional expansion of the out-of-plane lattice parameter of 0.6–4.1% is observed.

Subsequent study of film stoichiometry using X-ray photoelectron spectroscopy (XPS) and Rutherford backscattering spectrometry (RBS) (see Experimental Section) reveals that all films possess nominally stoichiometric cation ratios within the limits of experimental error (+/−1%) (Supporting Information, Figure S2). This observation is consistent with prior studies of BaTiO$_3$,[31] but does not explain the observed increase of the out-of-plane lattice parameter. Oxygen post-annealing of the films results in no change in the lattice parameters, eliminating chemical expansion from isolated oxygen vacancies as the mechanism for the lattice expansion. Taken together, these results suggest that the lattice expansion observed with increasing laser fluence arises not from cation or anion compositional deviations, but from defects associated with the varying energetics of the growth process.[32,33] Such effects have been observed previously in the PLD growth of SrRuO$_3$[34] where expansions as large as 3.8% were observed. Despite reporting a direct connection between the expanded lattice constants and the energetic bombardment during deposition, the exact mechanism responsible for the lattice constant extension was not well understood. It was hypothesized that collision-induced displacement of cations into nonequilibrium lattice locations, implantation of the various ionic species during growth, resputtering of the film, and/or composition differences resulting from relative cation distributions in the laser plume, which are also pressure and fluence dependent, could be responsible. These observations highlight the incredible ability of complex oxide perovskites to accommodate and sustain large densities of point defects as both individuals and clusters, that in turn, are responsible for such dramatic changes in the lattice parameter of these materials from the ideal, bulk structure.[35–38]
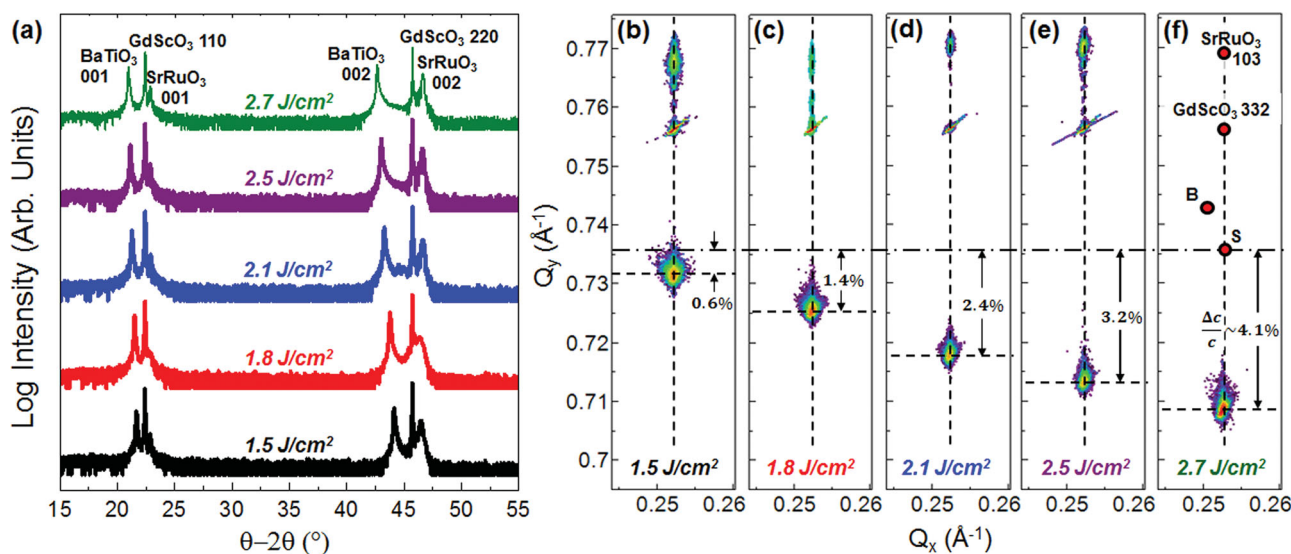

Figure 1. (a) θ-2θ X-ray diffraction studies of BaTiO$_3$/SrRuO$_3$/GdScO$_3$ (110) heterostructures where the BaTiO$_3$ film was grown at a laser fluence of (from bottom-to-top) 1.5, 1.8, 2.1, 2.5, and 2.7 J/cm^2. Corresponding off-axis reciprocal space mapping studies about the 103- and 332-diffraction conditions of the films and substrate for BaTiO$_3$ films grown at a laser fluence of (b) 1.5 J/cm^2, (c) 1.8 J/cm^2, (d) 2.1 J/cm^2, (e) 2.5 J/cm^2, and (f) 2.7 J/cm^2. Despite all films possessing the same in-plane lattice parameters, the out-of-plane lattice parameter is observed to increase with increasing laser fluence.
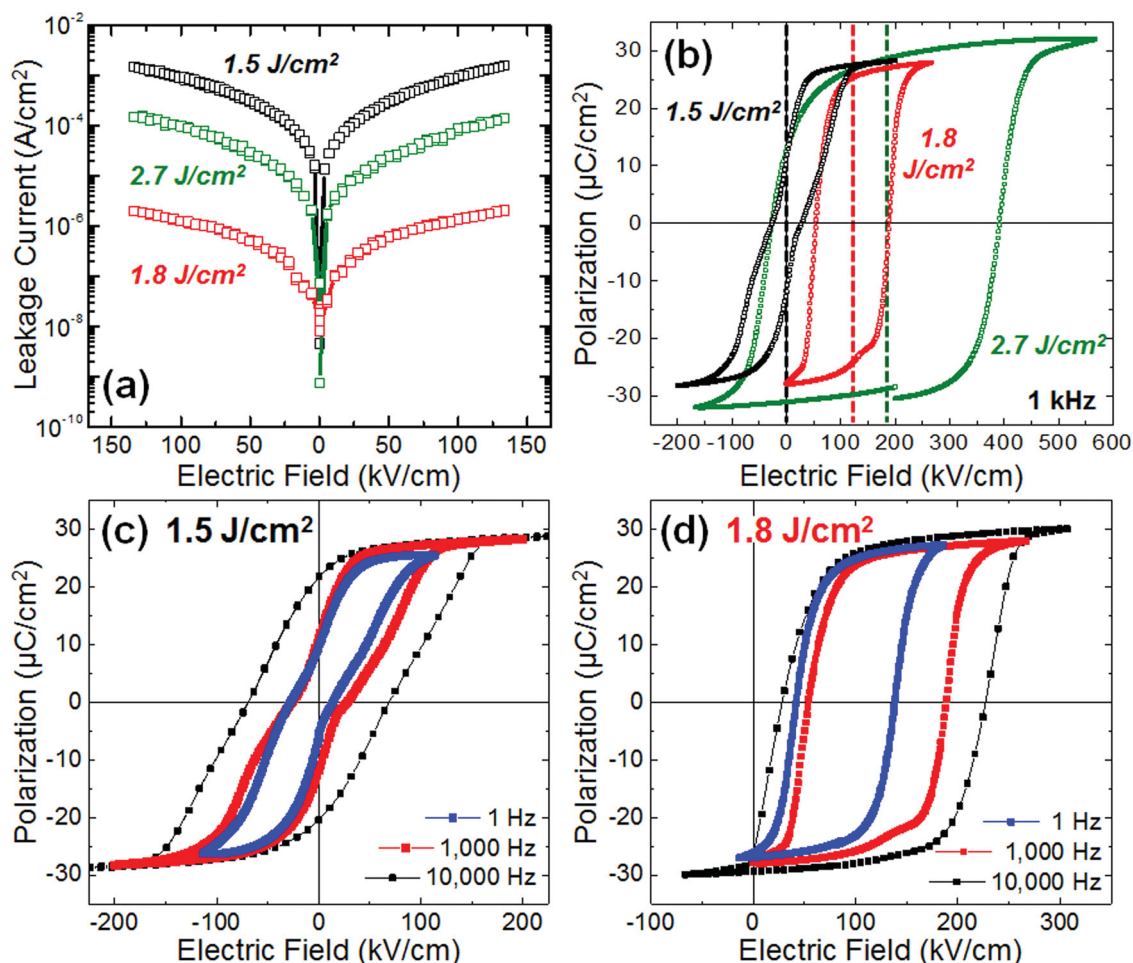
Materials
Views
www.MaterialsViews.com

ADVANCED
MATERIALS
www.advmat.de

COMMUNICATION

Figure 2. (a) Leakage current as a function of applied electric field for $BaTiO_3/SrRuO_3/GdScO_3$ (110) heterostructures grown at laser fluences of 1.5, 1.8, and 2.7 J/cm^2. (b) Ferroelectric hysteresis loops for the same heterostructures measured at 1 kHz revealing increasing shifts along the voltage axis with increasing laser fluence. Frequency-dependent polarization hysteresis loops for heterostructures with $BaTiO_3$ grown at (c) 1.5 J/cm^2 and (d) 1.8 J/cm^2. Films grown at lower fluences show horizontally centered, but pinched loops while those grown at higher fluence reveal shifted, but unpinched loops.

To gain further insight into the nature of these growth-induced defects and their impact on ferroelectricity, detailed ferroelectric characterization was completed (see Experimental Section). Ferroelectric hysteresis loops were obtained from 0.001–10 kHz using symmetric $SrRuO_3$ capacitor structures[39] which suppress extrinsic metal-ferroelectric interface related effects including imprint, asymmetric leakage, and lossy dielectric responses.[40] Accordingly, the leakage characteristics (**Figure 2**a) for films grown at 1.5, 1.8, and 2.7 J/cm^2 on $GdScO_3$ (110) substrates reveal symmetric, low-current response. Of particular interest is the fact that the leakage in films grown at high fluences (1.8 and 2.7 J/cm^2) is one-to-two orders-of-magnitude lower than for the films grown at lower laser fluence (1.5 J/cm^2) suggesting that the growth induced defects that give rise to increased cell volume do not also give rise to increased leakage. Characteristic ferroelectric hysteresis loops measured at 1 kHz (Figure 2b) reveal two distinct behaviors: 1) horizontally centered, but pinched loops for films grown at 1.5 J/cm^2 (blue data, Figure 2b) and 2) horizontally-shifted, unpinched loops that exhibit shifts that scale with the laser fluence (1.8 and 2.7 J/cm^2, red and green data, respectively,

Figure 2b). Both of these features are signatures of the presence of defect dipoles that are aligned out-of-the-plane of the films.[41,42] Additional insight is gained by exploring the frequency dependent evolution of the hysteresis loops, here shown for films grown at 1.5 and 1.8 J/cm^2 (Figure 2c and d, respectively). Films grown at low laser fluence (1.5 J/cm^2) exhibit loops that are horizontally centered across all frequencies studied, but exhibit pinching when probed at frequencies <5 kHz. Films grown at higher laser fluences show no loop pinching across the range of frequencies studied, but become increasingly off-centered as the measurement frequency is increased. These results are consistent with previous studies of $Pb_{0.98}Ba_{0.02}(Mg_{1/3}Nb_{2/3})O_3$-$PbTiO_3$ where thin films grown under high-bombardment conditions possessed large internal electric fields giving rise to only a single stable state of remnant polarization that could not be switched.[43]

Such ferroelectric switching behavior (i.e., the presence of pinched/shifted hysteresis loops) and the observed lattice expansion substantiate the presence of growth-induced defect dipoles that increase in concentration with laser fluence. A defect dipole is a generic term referring to any defect-complex

that forms when two or more oppositely charged point defects in a lattice couple or interact in such a manner to produce a negative energy of association. In ferroelectrics, this typically refers to a complex of some acceptor defect and an oxygen vacancy or a donor defect and a cation vacancy.[16,27] While the exact nature of the acceptor (or donor) defect can vary, they are likely formed in the films in this study due to the energetic bombardment from the growth process, and are therefore predominantly from intrinsic point defects such as cation and anion vacancies (and potentially interstitials or anti-site defects). It should also be noted that the formation of such defect dipoles is also likely related to the observed reduction in leakage currents as they compensate for oxygen vacancies or serve as trap states for free carriers in the film.

In turn, the expansion of the out-of-plane lattice parameter and the shift in the hysteresis loop are thought to be related to the elastic- and electric-dipole moments of the defect dipoles, respectively.[27] The effect of the latter is well characterized in the literature as the coupling between the electric-dipole moment and the spontaneous polarization of the ferroelectric is known to break the degeneracy of the up/down polarization states (i.e., giving rise to local built-in fields that pin the ferroelectric polarization and result in shifted and pinched loops). Shifted loops are expected when all of the defect dipoles are aligned and pinched loops when there is a mixture of up- and down-oriented defect dipoles. Likewise, the lattice distortion associated with the elastic-dipole depends on the orientation of the defect dipole and the net lattice deformation is proportional to the number of dipoles aligned in any direction.[25,27] It is known that external stresses can also break the degeneracy between symmetrically equivalent orientations of the elastic dipoles.[25,26] The BaTiO₃ films exhibit large expansion in the out-of-plane lattice parameter, while the in-plane lattice parameters remain constrained to that of the underlying GdScO₃ substrate, suggesting that the strain field from the (compressive) epitaxial strain can produce similar out-of-plane alignment of the defect dipoles. The idea that stress (or strain) can drive the alignment of defect dipoles has been around for some time[27] and ultimately the electric and the elastic dipole energies can have different signs which can lead to complex alignment geometries. From our direct measurements of defect-dipoled-induced

lattice deformation and built-in internal fields, it is possible to estimate the realtive magnitude of the elastic and electric energies, respectively (see Supporting Information). The elastic energy associated with alignment of the defect dipoles is found to be at least an order of magnitude larger than that from electrical alignment alone. This suggests that both the orientation and stability of the defect-dipole alignment are impacted not just by the electric coupling, but by a strong elastic coupling. Such observations are consistent with work that showed alignment of paramagnetic Na⁺-O⁻ dipoles in BaTiO₃ crystals under the application of a uniaxial mechanical stress.[44]

To further probe this idea, samples were grown at a laser fluence of 1.8 J/cm² on a range of different substrates including DyScO₃ (110), GdScO₃ (110), and NdScO₃ (110). Consistent with the films described above, all films are coherently strained to the various substrates and as one moves from films grown on NdScO₃ to GdScO₃ to DyScO₃ the out-of-plane lattice parameter of the BaTiO₃ increases as is expected based on the changing strain condition (Supporting Information, Figure S3). Subsequent hysteresis loop measurements (**Figure 3**a and b, measured at 1 Hz and 10 kHz, respectively) reveal that films grown on substrates that provide a compressive strain (i.e., DyScO₃ and GdScO₃) exhibit large horizontal shifts of the hysteresis loops indicating built-in fields arising from aligned defect dipoles while films grown on substrates that provide a small tensile strain (i.e., NdScO₃) reveal negligible built-in fields suggesting that the defect dipoles are not preferentially aligned in the out-of-plane direction. Again, this data suggests that the epitaxial strain plays a crucial role in directing the out-of-plane alignment of the defect dipoles and the observation of built-in fields. As the elastic boundary conditions are changed from compressive to tensile in nature, we see clear trends (i.e., increasing shifts of the hysteresis loop with increasing compressive strain) that suggest that epitaxial strain, not just polarization, are key to understanding the alignment of the defect dipoles.

So far we have demonstrated that compressive epitaxial strain can drive an out-of-plane alignment of growth-induced defect dipoles that manifest structurally as large expansions in the c-axis lattice parameter of the films. Such deformations signify the presence of large internal-stresses in the out-of-plane
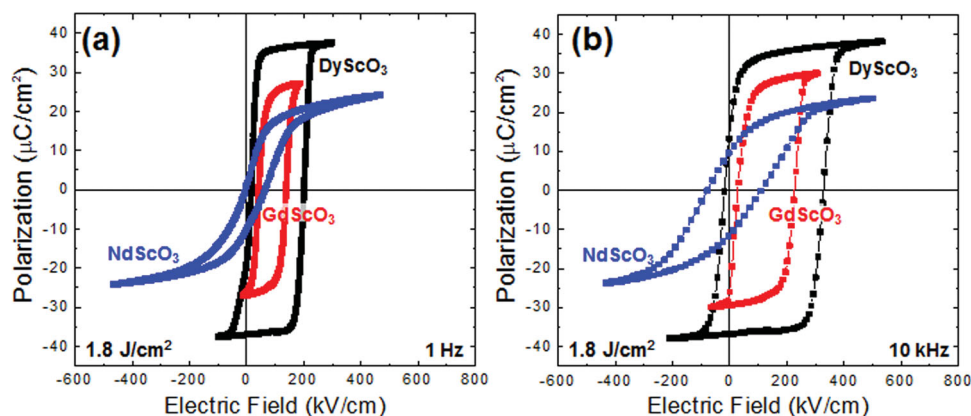

Figure 3. Polarization electric field hysteresis loops for BaTiO₃/SrRuO₃ heterostructures grown at a laser fluence of 1.8 J/cm² on substrates producing a compressive (SrTiO₃ and GdScO₃) and tensile (NdScO₃) epitaxial strain as measured at (a) 1 Hz and (b) 10 kHz. A change in the sign of the strain results in a change in the nature of the loops with compressive strains driving shifted loops and tensile strains resulting in no shifts.
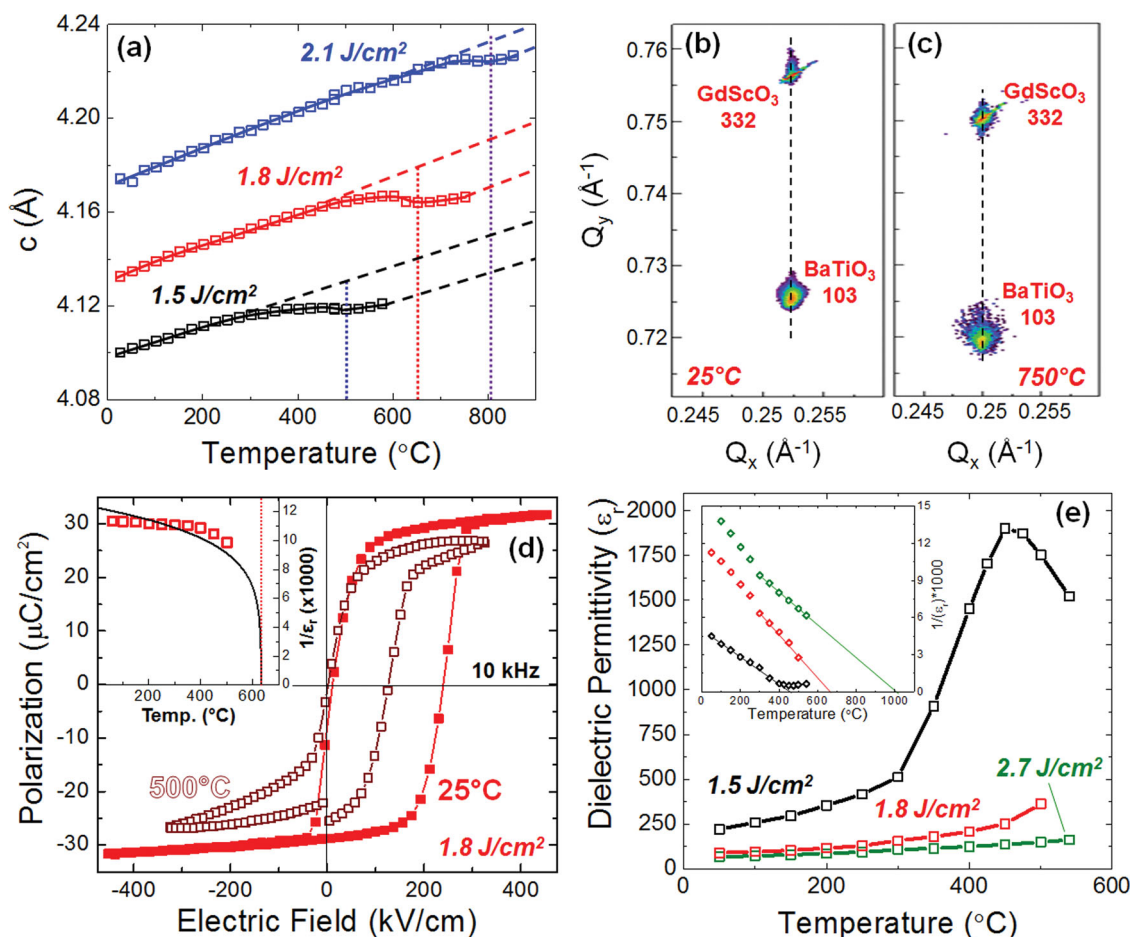
Materials
Views
www.MaterialsViews.com

ADVANCED
MATERIALS
www.advmat.de

COMMUNICATION

Figure 4. (a) Temperature-dependence of out-of-plane c-axis lattice parameter as measured from X-ray diffraction for $BaTiO_3/SrRuO_3/GdScO_3$ (110) heterostructures where the $BaTiO_3$ was grown at laser fluences of 1.5 (black), 1.8 (red), and 2.1 (blue) J/cm^2. Two distinct regimes, separated by a kink in the lattice parameter are observed. Corresponding X-ray reciprocal space mapping studies of the heterostructure grown at 1.8 J/cm^2 at (b) 25 °C and (c) 750 °C revealing that the films remain coherently strained even at high temperatures. (d) Ferroelectric hysteresis loops, measured at 10 kHz, for the heterostructure grown at 1.8 J/cm^2 revealing the presence of strong polarization even at 500 °C. The inset shows a summary of the evolution of the polarization from 25–500 °C. (e) Dielectric permittivity of $BaTiO_3$ films grown at laser fluences of 1.5 (black), 1.8 (red), and 2.7 (green) J/cm^2 measured as a function of temperature. The inset shows the inverse permittivity as a function of temperature a linear fit of the high-temperature response to extract an estimate for the transition temperature.

direction that arise from the elastic interactions between the aligned defect-structures and the host lattice. It has been shown that the presence of lattice strains can dramatically impact the magnitude and temperature-dependence of the polar state in $BaTiO_3$.[28,45] In fact, researchers have shown that epitaxial strain alone can increase the T_C of $BaTiO_3/GdScO_3$ (110) heterostructures from 130 °C to 400 °C.[2] To explore the added effect of the out-of-plane lattice strains from the aligned defect dipoles on the T_C of $BaTiO_3$ films, we conducted temperature-dependent XRD studies of $BaTiO_3/SrRuO_3/GdScO_3$ (110) heterostructures grown at laser fluences of 1.5, 1.8, and 2.1 J/cm^2 (**Figure 4**a). The temperature-dependent evolution of the out-of-plane lattice parameter reveals two regimes of thermal expansion over the temperature range from 25–900 °C separated by a kink that is characteristic of a phase transition. RSM studies were completed at various temperatures throughout these studies and, in all cases, the films were found to remain coherently strained to the substrate [characteristic data for films

grown at 1.8 J/cm^2 are provided for studies at 25 °C (Figure 4b) and 750 °C (Figure 4c)]. Subsequently, from the evolution of the out-of-plane lattice parameter, the presence of phase transitions at ~500 °C, ~650 °C, and ~800 °C for films grown at laser fluences of 1.5, 1.8, and 2.1 J/cm^2, respectively, are suggested. We also note that the excess lattice deformation (beyond that resulting from epitaxial strain) associated with the defect dipoles is observed to persist to even above the phase transition temperature which is further proof that the defect dipoles are coupled strongly to the epitaxial strain state of the films.

To verify that the structural transitions observed in the XRD studies correspond to the transition from a ferroelectric-to-paraelectric state, we probed the temperature dependence of the dielectric and ferroelectric properties. To begin, we show data for the temperature-dependent evolution of spontaneous polarization for a film grown at 1.8 J/cm^2 (Figure 4d). Ferroelectric hysteresis loops were obtained up to 500 °C and reveal a spontaneous polarization value of 27 $\mu C/cm^2$ (~80% of the

room-temperature value) despite being 100 °C above the T_C for a defect-free, coherently strained film.[2] This suggests that the stabilization of the ferroelectric state of BaTiO$_3$ from aligned defect dipoles can dramatically impact the properties. The temperature dependence of the ferroelectric polarization (inset, Figure 4d) is provided to summarize the response from 25–500 °C. To further explore the mechanism for the enhancement of T_C, we employed Ginzburg-Landau-Devonshire (GLD) models[46] to predict the temperature evolution of the spontaneous polarization considering both the out-of-plane elastic strain arising from aligned defect-dipoles and the in-plane biaxial epitaxial strain from the substrate (Supporting Information, Figure S6). The predicted temperature dependence of the spontaneous polarization for the film grown at 1.8 J/cm^2 matches closely with the experimentally measured values (inset, Figure 4d) and suggests a phase transition at T_C ≈650 °C that coincides with the phase transition observed in the temperature-dependent XRD. Likewise, the predicted T_C for films grown at 1.5, 2.1, and 2.7 J/cm^2 are ≈515 °C, ≈810 °C, and 1083 °C respectively; in excellent agreement with the temperature-dependent XRD (Figure 4a) and strongly suggesting that the anomalies in the XRD studies correspond to ferroelectric-to-paraelectric transitions. These observations also lead us to conclude that these enhancements in the T_C can be attributed to the epitaxial strain-induced alignment of growth-induced defect dipoles that in turn produce anisotropic lattice deformations and enhanced strain states.

Further insight into the ferroelectric nature of these transitions is obtained from temperature-dependent dielectric measurements (Figure 4e) for the films grown at 1.5, 1.8, and 2.7 J/cm^2. Fits of the inverse dielectric response as a function of temperature (inset, Figure 4e) for these films suggest T_C ≈475 °C, 650 °C, and 1000 °C for films grown at 1.5, 1.8, and 2.7 J/cm^2, respectively. These values are in excellent agreement with the predictions from the GLD models which can be used to predict the T_C for a given combination of epitaxial and defect dipole strain. Moreover, in the case of the films grown at a fluence of 1.5 J/cm^2, we observe a sharp dielectric anomaly through the structural transition ~475 °C (black data, Figure 4e) confirming the presence of a ferroelectric-to-paraelectric phase transition at this temperature. Additional details of the dielectric permittivity and ferroelectric properties before and after temperature cycling are also provided (Supporting Information, Figures S4 and S5).

In summary, we have explored the coupling between epitaxial strain and defect dipoles that form due to the PLD growth process to controllably tune the T_C of BaTiO$_3$ to over 800 °C. Purely epitaxial strain-based approaches for T_C enhancement are limited by the magnitude of strain that can be applied, the thicknesses that can be achieved before film relaxation, and a lack of strain tunability. In this work we show that epitaxial strain can be used to control the ordering of defect dipoles inducing additional out-of-plane strains and enabling controlled enhancement of T_C without the need to change substrates. This is especially exciting since neither the polarization nor the leakage properties are diminished thereby enabling the measurement of well-defined ferroelectric hysteresis loops to at least 500 °C. It should be noted that even in bulk crystals, aging (a time dependent alignment of defect complexes in the

direction of polarization) can give rise to enhanced T_C, but the exact mechanism was not well understood nor is it known how to deterministically control the magnitude and nature of these effects.[47] Additionally, in bulk materials the enhancement of T_C has also been observed to be fleeting or time-dependent, but our enhanced properties have been observed to be stable for > 6 months likely due to the added stabilizing power of the epitaxial constraints. Such a combined control of epitaxial strain and growth-induced defect-structures to control ferroelectricity in materials opens up a new paradigm in strain control of properties. We note, however, that this is not the first time that the growth process has been used to manipulate the density of defects in a material. In fact, in group IV semiconductors (e.g., Si$_x$Ge$_{1-x}$) it has been shown that ion-assisted deposition methods can produce defect complexes that can be used to modify the strain state of materials.[48] Early work in this capacity even lead some researchers to suggest that "strain 'engineering' by controlled ion beam defect injection may have interesting implications for lattice-mismatched heteroepitaxy" and may lead to the accommodation "of film-substrate lattice mismatch in a novel manner."[48] Our work provides a new application of this concept to complex oxide ferroelectrics and represents an exciting discovery with implications for utilization of these materials in high-temperature applications.

Experimental Section

BaTiO$_3$ Film Growth: Epitaxial 130–170 nm BaTiO$_3$/40 nm SrRuO$_3$ heterostructures were grown on DyScO$_3$ (110), GdScO$_3$ (110) and NdScO$_3$ (110) single-crystal substrates (Crystec, GmbH) via pulsed-laser deposition (PLD) using a KrF excimer laser (LPX 205, Coherent). The BaTiO$_3$ films were grown in 20 mTorr of oxygen at 600 °C from a BaTiO$_3$ ceramic target at a laser repetition rate of 2 Hz while the laser fluence was varied between 1.5 and 2.7 J/cm^2. The SrRuO$_3$ bottom electrode was grown in 100 mTorr of oxygen at 640 °C from a SrRuO$_3$ ceramic target at a laser repetition rate of 17 Hz and a laser fluence of 1.5 J/cm^2. In both cases, the targets were sanded, cleaned, and sufficiently preablated to assure the target surface had reached steady state prior to growth. For all films the growth took place in an on-axis geometry with a target-to-substrate separation of 6.6 cm. Following the growths, the films were cooled to room temperature at 5 °C/min. in a 760 Torr oxygen pressure.

Chemical Analysis: X-ray photoelectron spectroscopy (XPS) was performed using a Kratos Axis XPS with a monochromatic Al X-ray source with charge neutralization during collection via electron beam bombardment at an emission angle of 0° from the surface normal. Analysis focuses on the XPS spectra of the Ti 2p edges of BaTiO$_3$ films grown at various laser fluences as well as the XPS spectra of a BaTiO$_3$ single crystal used to calibrate the composition. Composition was measured and calculated using the CasaXPS software. Rutherford backscattering spectrometry (RBS) was performed with an incident ion energy of 2000 keV, incident angle $\alpha = 22.5°$, exit angle $\beta = 52.5°$, and a scattering angle $\theta = 150°$. RBS studies were completed on BaTiO$_3$ films grown on YAlO$_3$ (110) substrates using the same growth conditions (and grown concurrently) with the films herein. This was done for ease of fitting and to allow for the most accurate probe of the Ba and Ti peaks in the RBS spectra with minimal overlap from the substrate peaks. The fits reported here were completed using the built-in fitting program in the RBS analysis software SIMNRA (simnra.com).

Dielectric and Ferroelectric Properties: The dielectric permittivity was extracted from the measured capacitance (C) using $C = \frac{\varepsilon_0 \varepsilon_r A}{d}$ where A is the area of the capacitor and d is the thickness of the film. Prior to measurement, the films were poled with a negative bias and films were measured at remanence. The dielectric permittivity as a function of

frequency was measured with an ac excitation voltage of 5–10 mV (rms) (corresponding to a field of 0.3–0.6 kV/cm). Ferroelectric hysteresis loops were measured using a Radiant Multiferroics Tester as a function of frequency from 0.001 – 20 kHz.

Supporting Information

Supporting Information is available from the Wiley Online Library or from the author.

Acknowledgements

[1] D. G. Schlom, L.-Q. Chen, C.-B. Eom, K. M. Rabe, S. K. Streiffer, J.-M. Triscone, *Annu. Rev. Mater. Res.* **2007**, *37*, 589.

[2] K. J. Choi, M. Biegalski, Y. L. Li, A. Sharan, J. Schubert, R. Uecker, P. Reiche, Y. B. Chen, X. Q. Pan, V. Gopalan, L.-Q. Chen, D. G. Schlom, C. B. Eom, *Science* **2004**, *306*, 1005.

[3] S. A. Harrington, J. Zhai, S. Denev, V. Gopalan, H. Wang, Z. Bi, S. A. T. Redfern, S.-H. Baek, C. W. Bark, C.-B. Eom, Q. Jia, M. E. Vickers, J. L. MacManus-Driscoll, *Nat. Nanotechnol.* **2011**, *6*, 491.

[4] J. H. Haeni, P. Irvin, W. Chang, R. Uecker, P. Reiche, Y. L. Li, S. Choudhury, W. Tian, M. E. Hawley, B. Craigo, A. K. Tagantsev, X. Q. Pan, S. K. Streiffer, L.-Q. Chen, S. W. Kirchoefer, J. Levy, D. G. Schlom, *Nature* **2004**, *430*, 758.

[5] R. J. Zeches, M. D. Rossell, J. X. Zhang, A. J. Hatt, Q. He, C.-H. Yang, A. Kumar, C. H. Wang, A. Melville, C. Adamo, G. Sheng, Y.-H. Chu, J. F. Ihlefeld, R. Erni, C. Ederer, V. Gopalan, V. Gopalan, L.-Q. Chen, D. G. Schlom, N. A. Spaldin, L. W. Martin, R. Ramesh, *Science* **2009**, *326*, 977.

[6] V. M. Mukhortov, Yu. I. Golovko, Vl. M. Mukhortov, V. P. Dudkevich, *Sov. Phys. J.* **1981**, *24*, 102.

[7] V. M. Mukhortov, Yu. I. Golovko, V. A. Aleshin, E. V. Sviridov, Vl. M. Mukhortov, V. P. Dudkevich, E. G. Fesenko, *Phys. Stat. Sol. A* **1983**, *77*, K37.

[8] K. Abe, S. Komatsu, N. Yanase, K. Sano, T. Kawakubo, *Jpn. J. Appl. Phys.* **1997**, *36*, 5575.

[9] T. Kawakubo, S. Komatsu, K. Abe, K. Sano, N. Yanase, N. Fukushima, *Jpn. J. Appl. Phys.* **1998**, *37*, 5108.

[10] D. Fu, K. Fukamachi, N. Sakamoto, N. Wakiya, H. Suzuki, M. Itoh, T. Nishimatsu, arXiv: 1102.4473 (22 Feb **2011**).

[11] J. Sinsheimer, S. J. Callori, B. Ziegler, B. Bein, P. V. Chinta, A. Ashrafi, R. L. Headrick, M. Dawber, *Appl. Phys. Lett.* **2013**, *103*, 242904.

[12] S. Tinte, K. M. Rabe, D. Vanderbilt, *Phys. Rev. B* **2003**, *68*, 144105.

[13] N. Yanase, K. Abe, N. Fukushima, T. Kawakubo, *Jpn. J. Appl. Phys.* **1999**, *38*, 5305.

[14] K. Abe, N. Yanase, T. Yasumoto, T. Kawakubo, *J. Appl. Phys.* **2002**, *91*, 323.

[15] S. V. Kalinin, A. Borisevich, D. Fong, *ACS Nano* **2012**, *6*, 10423.

[16] D. Damjanovic, *Rep. Prog. Phys.* **1998**, *61*, 1267.

[17] S. Lee, C. A. Randall, *J. Am. Ceram. Soc.* **2008**, *91*, 1748.

[18] S. Lee, C. A. Randall, *J. Am. Ceram. Soc.* **2008**, *91*, 1753.

[19] Y. Sakabe, H. Takgi, *Jpn. J. Appl. Phys.* **2002**, *41*, 6461.

[20] S. B. Majumder, Y. N. Mohapatra, D. C. Agrawal, *Appl. Phys. Lett.* **1997**, *70*, 138.

[21] S. Zhang, R. E. Eitel, C. A. Randall, T. R. Shrout, E. F. Alberta, *Appl. Phys. Lett.* **2005**, *86*, 262904.

[22] X. Ren, *Nat. Mater.* **2004**, *3*, 91.

[23] D. Lee, B. C. Jeon, S. H. Baek, S. M. Yang, Y. J. Shin, T. H. Kim, Y. S. Kim, J.-G. Yoon, C.-B. Eom, T. W. Noh, *Adv. Mater.* **2012**, *24*, 6490.

[24] W. Hu, Y. Liu, R. L. Withers, T. J. Frankcombe, L. Noren, A. Snashall, M. Kitchin, P. Smith, B. Gong, H. Chen, J. Schiemer, F. Brink, J. Wong-Leung, *Nat. Mater.* **2013**, *12*, 821.

[25] A. S. Nowick, W. R. Heller, *Adv. Phys.* **1963**, *12*, 251.

[26] R. Balzer, H. Peters, W. Waidelich, *Phys. Rev. B* **1974**, *9*, 2746.

[27] G. Arlt, H. Neumann, *Ferroelectrics* **1988**, *87*, 109.

[28] C. Ederer, N. A. Spaldin, *Phys. Rev. Lett.* **2005**, *95*, 257601.

[29] T. Ohnishi, M. Lippmaa, T. Yamamoto, S. Meguro, H. Koinuma, *Appl. Phys. Lett.* **2005**, *87*, 241919.

[30] E. Breckenfeld, R. Wilson, J. Karthik, A. R. Damodaran, D. G. Cahill, L. W. Martin, *Chem. Mater.* **2012**, *24*, 331.

[31] D. S. Kan, Y. Shimakawa, *Appl. Phys. Lett.* **2011**, *99*, 081907.

[32] P. R. Willmott, J. R. Huber, *Rev. Mod. Phys.* **2000**, *72*, 315.

[33] J. Perrière, E. Millon, W. Seiler, C. Boulmer-Leborgne, V. Craciun, O. Albert, J. C. Loulergue, J. Etchepare, *J. Appl. Phys.* **2002**, *91*, 690.

[34] J.-P. Maria, S. Trolier-McKinstry, D. G. Schlom, M. E. Hawley, G. W. Brown, *J. Appl. Phys.* **1998**, *83*, 4373.

[35] H. L. Tuller, S. R. Bishop, *Annu. Rev. Mater. Res.* **2011**, *41*, 369.

[36] D. M. Smyth, *Annu. Rev. Mater. Sci.* **1985**, *15*, 329.

[37] A. Pramanick, A. D. Prewitt, J. S. Forrester, J. L. Jones, *Critical Reviews in Solid State and Materials Sciences* **2012**, *37(4)*, 243.

[38] E. Breckenfeld, A. B. Shah, L. W. Martin, *J. Mater. Chem. C* **2013**, *1*, 18052.

[39] J. Karthik, A. R. Damodaran, L. W. Martin, *Adv. Mater.* **2010**, *24*, 1610.

[40] N. Setter, D. Damjanovic, L. Eng, G. Fox, S. Gevorgian, S. Hong, A. Kingon, H. Kohlstedt, N. Y. Park, G. B. Stephenson, I. Stolitchnov, A. K. Taganstev, D. V. Taylor, T. Yamada, S. Streiffer, *J. Appl. Phys.* **2006**, *100*, 051606.

[41] G. E. Pike, W. L. Warren, D. Dimos, B. A. Tuttle, R. Ramesh, J. Lee, V. G. Keramidas, J. T. Evans Jr., *Appl. Phys. Lett.* **1995**, *66*, 484.

[42] W. L. Warren, G. E. Pike, K. Vanheusden, D. Dimos, B. A. Tuttle, J. Robertson, *J. Appl. Phys.* **1996**, *79*, 9250.

[43] J.-P. Maria, J. F. Shepard Jr., S. Trolier-McKinstry, T. R. Watkins, A. E. Payzant, *Int. J. Appl. Ceram. Technol.* **2005**, *2(1)*, 51.

[44] T. Varnhorst, O. F. Schirmer, H. Kröse, R. Scharfschwerdt, Th. W. Kool, *Phys. Rev. B* **1996**, *53*, 116.

[45] H. Wu, G. Chai, B. Xu, J. Li, *Appl. Phys. A* **2013**, *113*, 155.

[46] A. F. Devonshire, *Philos. Mag.* **1951**, *42*, 1065.

[47] D. Sun, X. Ren, K. Otsuka, *Appl. Phys. Lett.* **2005**, *87*, 142903.

[48] C. J. Tsai, P. Rozenak, H. A. Atwater, T. Vreeland, *J. Cryst. Growth* **1991**, *111*, 931.